IRSTI 53.01.97 https://doi.org/10.26577/phst.2020.v7.i1.03

Electrochemical determination of corrosion protection and phase composition of nitride layers on steels

E. Lunarska[1*], R. Atchibayev[1] and J. Z. Michalski[2]

[1]*Institute of Physical Chemistry, Polish Academy of Sciences, 44/52, Kasprzaka Str., 01-224 Warsaw, Poland*
[2] *Institute of Precision Mechanics, 3, Duchnicka Str., 01-796, Warsaw, Poland*
**e-mail: elina.lunarska@edu.pl*

Electrochemical method providing the possibility to check the penetrating porosity, corrosion resistance and phase composition of nitrided surface has been developed and applied for high-speed SW18 steel nitrided from plasma excited H_2 +N_2 gas mixture and for structural 10A and 45A steels nitrided from NH_3 gas dissociated at different parameters. By selection the appropriate electrolytes, the phase composition of nitrided layer in SW18 steel, and the corrosion resistance of ε or γ' compact nitride layer on 10A and 45A steels have been evaluated and confirmed by material science and corrosion tests. Electrochemical methods may be applied to control the quality of obtained nitrided layer, and to correct or modify the program of technological process. Electrochemical method provided the possibility to check the penetrating porosity, corrosion resistance and phase composition of nitrided surface By selection the appropriate electrolytes, the phase composition and the corrosion resistance of nitride layers formed on SW18, 10A and 45A steels were established in accordance with the material investigation and corrosion tests data.

Key words: high speed SW18 steel, 10A steel, 45A steel, plasma nitriding, γ' phase, ε phase, H_3P0_4, borate, NaCl.
PACS number: 81.40.Np.

1 Introduction

Nitriding has been commonly used to increase the hardness, wear resistance, and the corrosion resistance of steels. Depending on steel composition and the kind and parameters of nitriding process, the surface layers consisting of diffusion zone, zones of compact γ, γ', ε nitrides or their mixture, as well as the carbo-nitrides may be formed. Transformation of carbides to carbo-nitrides, presence of porous e nitride or non-porous y' nitride layer affect the corrosion resistance. Using the modem facilities and the computer control of process (especially the nitriding potential and the heating rate) the layers of various phase composition and structure may be obtained [1-4]. In order to control the quality of obtained layer, and to correct or modify the program of technological process, the express method for determining the properties and composition of nitrided layer should be elaborated and applied. This possibility provides the electrochemical methods. Application of potentistatic or potentidynamic electrochemical tests allows to establish the phase (or chemical) composition of nitrided surface [5-9], to measure the penetrating porosity of the surface layer [10-16] and to evaluate the comparative corrosion resistance of nitrided steel in various environments.

In present work, the results of potentiodynarnic tests done in selected electrolytes enabling to check the corrosion resistance and the phase composition of nitrided layers formed under conditions providing the various nitride phase composition are shown.

Chemical composition of used high speed SW18 and structural 10A and 45A steels is shown in Table 1. Structural steels were nitrided from NH_3 gas phase, in a stepwise process. Specimens were heated at 450°C in pure, non dissociated NH_3 and then for short time in the 100% dissociated NH3. In a next step, nitriding proceeded at 490°C in the gas

containing mixture of 45%: 55% of dissociated to non dissociated NH_3 (process N40) and the mixture of 38% : 62% dissociated to non dissociated NH_3 (process N60). The final step of nitriding was done at parameters shown in Table 1. As a result, the compact nitride layers consisting on ε (process N40) and of γ'+ε (process N60) of thickness shown in Table 1, have been obtained. At nitriding of high-speed SW18 steel in a plasma excited gas mixture at parameters shown in Table 1, the nitride layer exhibiting only diffusion zone of different thickness was obtained.

Table 1 – Studied steel composition and the parameters of mitriding processes

Steel	Specim en code	Parameters of nitriding process	Nitriding layer structure	Nitriding layer thickness, pm
10A 0.1C, 0.5Mn,0.3Si,0.05Cr	N40	530°C, NH_3:NH_3dys=40:60, 4h	compact ε	6
as above	N60	530°C, NH_3:NH_3dys=57:43, 4h	compact (γ` + ε)	7
45A 0.46C, 0.7Mn. .28Si,0.08Cr	N40	530°C, NH,:NH_3dys=40:60. 4h	compact ε	4
as above	N60	530°C, NH_3:NH_3dys=57:43, 4h	compact (γ`+s)	5
SW18 0.9C, 4.2Cr, 17.5W, 1.15V	N1	plasma assisted, 490°C, H_2:N,=3:1. 1h.	diffusion layer.	15
as above	N10	plasma assisted, 490°C, H,:N,=3:1. 10h	diffusion layer,	45

Polarization curves were recorded with a potential scan rate 1 mV/s, using microcell of working area 0.05 cm2, placed on the nitrided surface. The 20% H_3PO_4 and borate (0.024M $Na_2B_4O_7$ + 0.12M H_3BO_3) electrolytes [17-25] were selected in order to evaluate the phase composition of nitrided layer. The 3% NaCl was used to check the relative susceptibility of nitrided layers formed on low alloy structural steels to corrosion in Cl containing environments.

2 Results and discussion

Electrochemical results have been compared with the results of microscopic and SEM observations, microhardness measurements, X-ray and GDS analysis and with results of corrosion tests.

Figure 1 shows the examples of polarization curves obtained for SW18 steel, bare and after N1 nitriding. The broad active peak on polarization curve recorded in H_3PO_4 has been associated with the dissolution of solid solution (matrix) phase, while peaks E_3 and E_4 could be accounted by the presence of MC and M_6C carbides [2], respectively. Indeed, in a bare SW18 steel, the X-ray examination revealed the presence of those carbides. Nitriding of SW18 steel caused the shift of peaks E_3 and E_4 to more anodic potential and the formation of two new peaks (E_1 and E_2) on polarization curve. Figure 2 shows the position of peaks seen on polarization curves recorded in H_3PO_4 for SW18 steel, nitrided in N10 process, after consequent removing of the surface material. The data show the phase distribution along the depth of nitrided layer. Potentials E_3 and E_4 returned to the values, characteristic for bare steel, at a distance from surface, similar to thickness of nitrided layer, established by microscopic observation and microhardness measurements. The above results of electrochemical tests showed that in a course of nitriding of SW18 steel, the transformation of carbide to the carbo-nitrides occurred and the nitrides were formed.

Figures 3 to 5 show the polarization curves recorded in different solutions for structural steels, bare and nitrided at different parameters. For bare low carbon steel 10A, no E_3 and E_4 peaks were observed on polarization curves recorded in H_3P0_4 solution (Figure 3). This may support the assumption of attributing of those peaks, observed for SW18 steel (Figure 1) to the dissolution of MC and MC_6 carbides, since low carbon 10A steel did not contain such carbides. Nitriding of 10A and 45A steels did not eliminate the active dissolution peak, but decreased its height and reduced the potential range. The new peak could be distinguished on polarization curve for nitrided steel, at potential close to potential of E_1 and E**2** peaks seen in the case of nitrided SW18 steel (cf. Figures 1 and 2).

This indicated the association of new peak with nitrides, formed at nitriding process.

Polarization curve recorded in borate solution for bare structural steel (Figure 4) exhibited two active peaks (E_1 and E_3). After nitriding in both processes, the new peak (E_N) appeared within the passive region. At subsequent removing of nitrided layer, this peak disappeared, revealing that its nature has been associated with the dissolution of nitrides. Unfortunately, at recording polarization curves either in H_3P0_4 or in borate solution, the kind of nitrides (ε or γ'ones) could not be distinguished, and the further studies should be carried out.

As follows from the X-ray examination (Table 1), after N40 and N60 nitriding processes, steels were covered with layers consisting of γ' nitride and of mixture of ε and γ' nitrides, respectively. According to [1], in the first case the nonporous and in a latter case the porous layers can be formed. As seen in Figure 3. steel nitrided in N60 process exhibited in whole potential range, the higher current densities than that nitrided in N40 process, revealing the higher porosity of nitrided layer formed in process N60 and consisting of e and γ' nitrides, in accordance with [1]. The higher porosity of layer formed in process N60 may be supported by data shown in Figure 4. Polarization curve for N60 specimen exhibited higher current than N40 specimen and the presence of peaks E_1 and E_2 resembling the peaks seen on polarization curve for bare steel. Therefore, by recording the polarization curve, the relative penetrating porosity of nitrided layer can be evaluated.

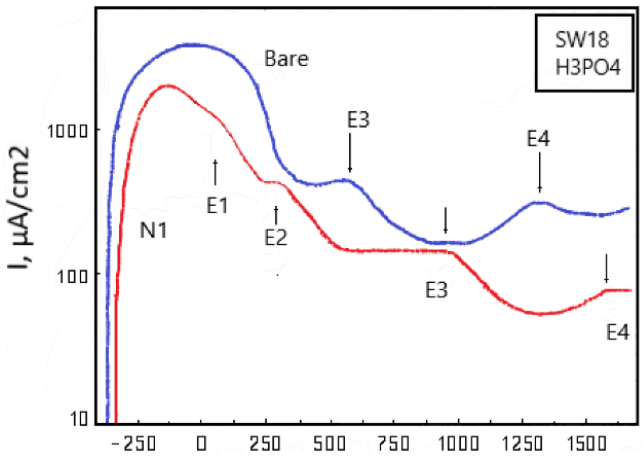

Figure 1 – Polarization curves recorded for SW18 steel, bare and after plasma assisted nitriding N1. Characteristic potentials associated with different carbides (carbo- nitrides) and nitride phase are marked

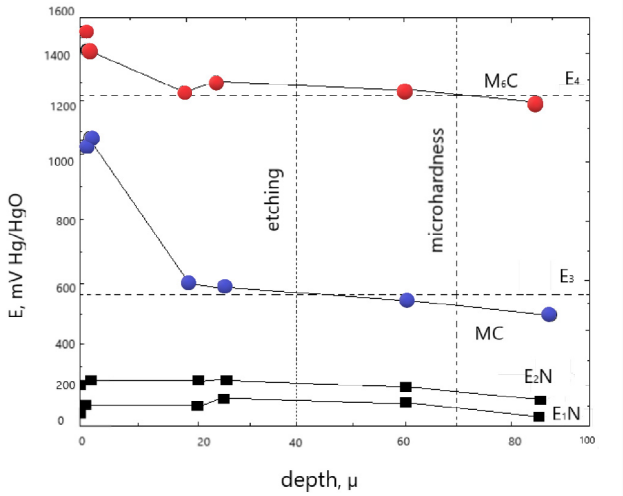

Figure 2 – Change of the position of characteristic potentials, associated with different phases of N10 nitrided SW18 steel along the distance from the specimen surface

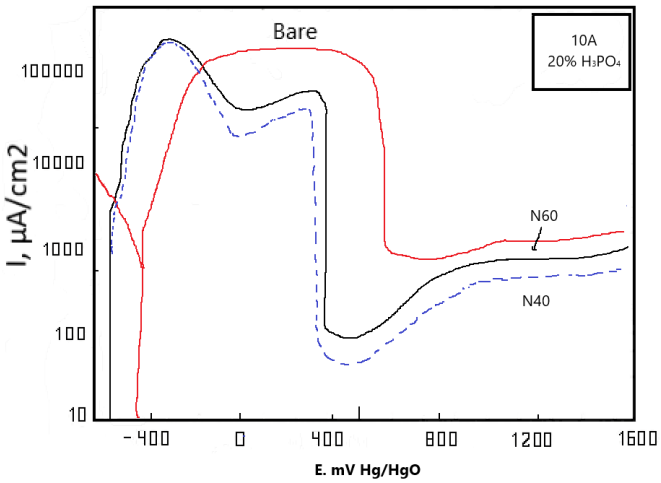

Figure 3 – Polarization curved for 10A steel, bare and nitrided under different conditions, recorded in H_3P0_4 solution

Bare structural steel exhibited the active dissolution at anodic polarization in NaCl solution, while nitriding caused the formation of a wide passive region, (Figure 5). The above results showed that the nitriding of structural steel with formation of compact nitride layer should drastically decrease the susceptibility to the corrosion in Cl containing solution. Those data were confirmed by the established in a special test susceptibility to pitting corrosion. At exposition in $FeCl_3$ solution, the higher number of pits of larger diameter was formed on bare, than on nitrided steel. The more extended passive region of lower passive current density in the case of N60 than N40 specimens (Figure 5) revealed the lower protection ability of layer formed in N40 process.

Those results seem to be in contrast to the results shown in Figures 3 and 4. However, in a pitting corrosion test, the steels subjected to N60 nitriding exhibited deeper pits than steels nitrided in N40 process. This indicated that the different parameters of nitride layer should be accounted for the penetrating porosity and for the passivation and resistivity to pitting corrosion in the Cl containing solutions.

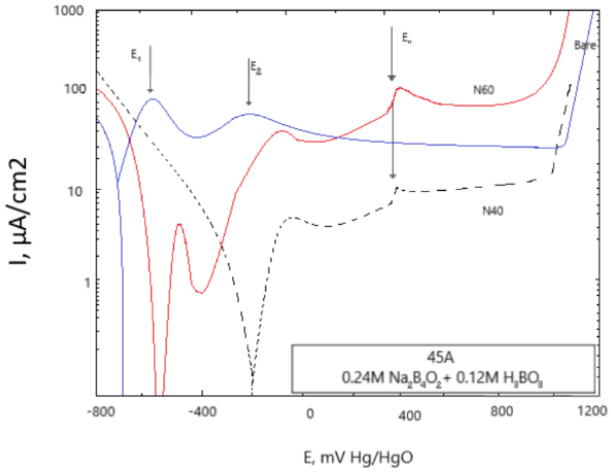

Figure 4 – Polarization curved for 45A steel, bare and nitrided under different conditions, recorded in borate solution

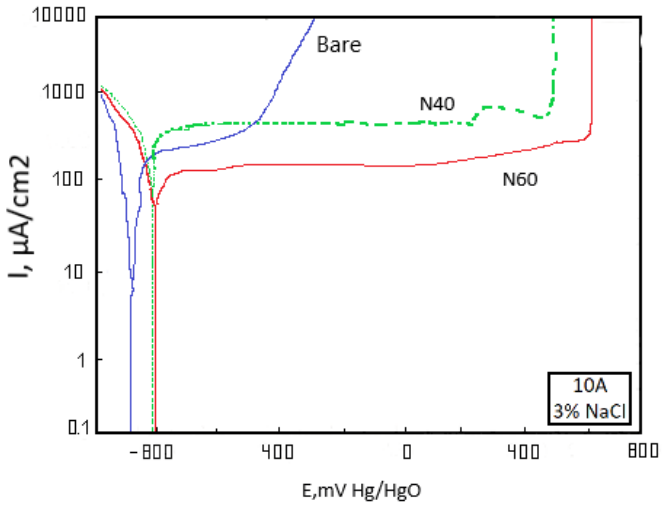

Figure 5 – Polarization curves for 10A steel, bare and nitrided under the different conditions, as recorded in NaCI solution.

3 Conclusions

Electrochemical method provided the possibility to check the penetrating porosity, corrosion resistance and phase composition of nitrided surface

By selection the appropriate electrolytes, the phase composition and the corrosion resistance of nitride layers formed on SW18, 10A and 45A steels were established in accordance with the material investigation and corrosion tests data.

References

1. Tacikowski I., Sutkowski I., Senatorski J., Michalski J. Modyfikowane warstwy azotowane wytwarzane w procesie regulowanym. porfczonym z utwardzaniem cieplnym podtoza // Inzynieria Materialowa. -2000. –V. 22. – P. 449-452. (in Polish).

2. Shapovalov E., Baranova L., Zektser G. Electrochemical methods in metallurgy and phase analysis. – Metalluggiya, Moscow. 2018. – 146 p. (in Russian).

3. Landolt D. Electrochemical methods for the characterization of PVD coatings // Proc. Intern. Congress of ISE-2000. Warsaw. Sept. 2015. – P. CD 3-22

4. Lunarska E., Nikiforow K. Okreslenie podatnosci na korozj wzerowa stali konstrukcyjnych a tym ze zmodyfikowan powierzchnrf / Ochrona przed Korozj. -2011. –V.44. – P. 1 15-119. (in Polish).

5. Karakurkchi A., Sakhnenko N., Atchibayev R. Research on the improvement of mixed titania and Co(Mn) oxide nano-composite coatings // IOP Conference Series: Materials Science and Engineering. -2018. – P. 69-74.

6. Ved' M., Sakhnenko N., Yermolenko I. Composition and corrosion behavior of iron-cobalt-tungsten // Eurasian Chemico-Technological Journal. -2018. -V.20(3).- P. 145-152.

7. Muradov A.D., Korobova N.E., Kyrykbaeva A.A. Influence of γ-iradiation on the optical properties of the polyimide–YBa2Cu3O6.7 system // Journal of Applied Spectroscopy. -2018. -V.85, – No.2.- P.260-266.

8. Yar-Mukhamedova G., Sakhnenko N. Nano-composition Ti-Co(Mn) coatings investigation // International Multidisciplinary Scientific GeoConference Surveying Geology and Mining Ecology Management, SGEM. -2018. –P. 1-15.

9. Darisheva A., Kasimzhanov K. Physicochemical investigations of scheelite concentrate decomposition // Eurasian Chemico-Technological Journal. -2015. –V. 7. – P. 209–212.

10. Muradov A., Korobova N. Impact of silver metallization and electron irradiation on the mechanical deformation of polyimide films // Technical Physics. -2017. -V. 62. – No. 11. –P. 1675–1678.

11. Belyaev, D. V., Mussabek, G., Sagyndykov, A. et.al. Modern state of composite coatings formation problem // 17th Int.l Multidisc. Sc Geoconf. SGEM 2017. 17 (61), -P 233-240.

12. Ved M.V., Karakurkchi A.V., Sakhnenko N.D.et al. Mixed alumina and cobalt containing plasma electrolytic oxide coatings // IOP Conference Series: Materials Science and Engineering. – 2017. – V. 213. – 6 p.

13. Ved M., Sakhnenko N., Koziar M. et al. Ternary cobalt-molybdenum-zirconium coatings for alternative energies // Applied Surface Science. 2017. -V. 384, – P. 56–65.

14. Yar-Mukhamedova G.Sh. Investigation of corrosion resistance of metallic composite thin-film systems before and after thermal treatment by the "corrodkote" method // Materials Science. -2001. -V.37, -No.1. – P.140-143.

15. Yermolenko I.Yu., Zyubanova S.I.et al. Surface analysis of Fe-Co-Mo electrolytic coatings. // IOP Conference Series: Materials Science and Engineering. – 2017. – P. 85-90.

16. Yar-Mukhamedova G., Ved' M., Sakhnenko N., Nenastina T. Electrodeposition and properties of binary and ternary cobalt alloys with molybdenum and tungsten // Applied Surface Science. -2018. -V. 445. –P. 298-307.

17. Aldabergenova T.M., Kislitsin S.B. et al. Effect of low-energy alpha-particles irradiation on surface structure and physical-mechanical properties of high-purity tungsten // AIP Conference Proceedings. 2016.

18. Sagyndykov A.B., Kalkozova Z.K. Fabrication of nanostructured silicon surface using selective chemical etching // Technical Physics. -2017. –V. 62(11). -Pp. 1692–1697.

19. Ghaferi Z., Sharafi S., Bahrololoom M.E. Effect of current density and bath composition on crystalline structure and magnetic properties of electrodeposited FeCoW alloy // Appl. Surf. Sci. -2015. –V. 355. –P. 766–773.

20. Bahlakeh G., Ramezanzadeh B., Saeb M.R., Terryn H., Ghaffari M. Corrosion protection properties and interfacial adhesion mechanism of an epoxy/polyamide coating applied on the steel surface decorated with cerium oxide nanofilm: Complementary experimental, molecular dynamics (MD) and first principle quantum mechanics (QM) simulation methods // Applied Surface Science. -2017. –V. 419. –P. 650-669.

21. Anicai L., Costovici S., Cojocaru A. et al. Electrodeposition of Co and CoMo alloys coatings using choline chloride based ionic liquids–evaluation of corrosion behavior // Int. J. of Surface Engineering and Coatings. -2015. –V. 93. –P. 302–312.

22. Mardani R., Shahmirzaee H., Mohammad H., Vahdani R. Electrodeposition of Ni32Fe48Mo20 and Ni52Fe33W15 alloy film on Cu microwire from ionic liquid containing plating bath // Surface and Coatings Technology. -2017. –V. 324. –P. 281–287.

23. Sakhnenko M.D., Ved' M.V., Ermolenko I.Yu. et al. Design, synthesis, and diagnostics of functional galvanic coatings made of multicomponent alloys // Mater. Sci., -2017. –V. 52(5). –P. 680–686.

24. Zhou H., Chen Z., Fang L. Pulse electroplating of Ni-WP coating and its anti-corrosion performance // Transactions of Nonferrous Metals Society of China. -2018. –V. 28(1). –P. 88–95.

25. Mehrizi S., Heydarzadeh M. Electrical resistivity and magnetic properties of electrodeposited nanocrystalline CoFe thin films // J. Mater. Sci.: Mater. Electron. – 2015. –V.26. –P. 7381–7389.